

Dualistic effect of the deformation of protective structures made of broken rock in mine workings under static load

Daria Chepiga^{1*}, Serhii Podkopaiev¹, Volodymyr Gogo¹, Oleksandr Shashenko²,
Oleksandr Skobenko², Oleksandr Demchenko³, Yevgen Podkopayev⁴

¹ Donetsk National Technical University, Luts'k, Ukraine

² Dnipro University of Technology, Dnipro, Ukraine

³ SE "Ukrshachthidrozakhyst", Kyiv, Ukraine

⁴ LLC MS YELTEKO, Kostyantynivka, Ukraine

*Corresponding author: e-mail daria.chepiha@donntu.edu.ua

Abstract

Purpose is to reveal physical essence of the dualistic (double) nature of deformation effects and their influence on the mechanical properties of protective structures made of broken rock while unloading coal-bearing mass to ensure stability of side rocks and operational conditions of the development mine working within the working areas of coal mines.

Methods. The deformation properties of protective structures made of broken rock was modeled on experimental samples during their static load in terms of uniaxial compression with the possibility of lateral expansion of the original material or its compressive stress.

Findings. A dualistic effect of deformations for the conditions of uniaxial compression of protective structures was revealed. Under the effect, a complex transformation of volume and shape occurs in the structures caused by the process of relative changes in the backfill material volume. The observed phenomenon occurs within the range of $0.12 \leq \delta V \leq 0.32$ and the values of the compaction coefficient of broken rock being $1.13 \leq k_{con.} \leq 1.47$, depending on the granulometric composition of the source material and its bulk density. It was established that under conditions when broken rock is compressed, there is an effect of forming the bearing capacity of protective structures, which is observed when a relative change in the volume of backfill material is $0.14 \leq \delta V \leq 0.38$, and its compaction factor reaches $1.16 \leq k_{con.} \leq 1.59$. Depending on the homogeneity degree of the backfill material of protective structures, when comparing the values of $k_{con.}$, a dualistic (double) effect is manifested in the difference of deformation characteristics of broken rock under uniaxial and compressive stress, reaching two or more times.

Originality. A regularity was established that determines the relationship between compaction factor $k_{con.}$ of broken rock and a relative change in the volume (δV) of backfill material, which makes it possible to evaluate bearing capacity of protective structures, being under static load in a stress-strain state.

Practical implications. The research results can be used to substantiate the selection of a method to protect development mine working with flexible supports made of broken rock. To clarify the assessment of bearing capacity of such structures, it is advisable to carry out specific field studies in mine conditions.

Keywords: protective structure, mine working, static load, deformation, rock, bearing capacity

1. Introduction

Coal mining and coal processing enterprises generate a large amount of solid waste sent to the surface and stored in dumps. Waste dumps are the main source of environmental pollution in coal-mining areas. The output and processing of mining mass and rock from the construction (54%) and repair (46%) of mine workings affects significantly the economic results of coal enterprises. About 50% of the surface and 60% of the underground transport of coal mines is used to bring rock to the surface.

Leaving rock in mines will solve the problem of waste-free environmentally safe production associated with the use of barren rocks as backfill materials. It is a promising

direction for utilization of rock dumps to place them in the underground mine workings of either operating mines or the ones being closed down [1], [2]. This approach will prevent caving of the mined-out space, reduce deformations of surface objects, and improve the environment in general. Basing on this fact, there is an urgent scientific task of developing and substantiating possible directions for the use of mine rock as backfill materials.

One of the effective ways of controlling rock pressure in coal-bearing masses is backfilling of a mined-out space. The use of this method favours reduction of harmful manifestations of rock pressure in stopings [2]. This method ensures stability of the development mine workings and prevents undermining of the earth's surface. Backfilling of a mined-

Received: 8 March 2024. Accepted: 12 June 2024. Available online: 30 June 2024

© 2023. D. Chepiga et al.

Mining of Mineral Deposits. ISSN 2415-3443 (Online) | ISSN 2415-3435 (Print)

This is an Open Access article distributed under the terms of the Creative Commons Attribution License (<http://creativecommons.org/licenses/by/4.0/>), which permits unrestricted reuse, distribution, and reproduction in any medium, provided the original work is properly cited.

out space helps reduce coal losses in mines and prevents their spontaneous ignition. The use of rock in mines for backfilling or construction of rock packs allows solving numerous technical problems [2]. The following are among them: prevention of caving of mine workings, cost reduction for their repair, and creating conditions for their repair-free maintenance. Determining the parameters of protective structures makes it possible to identify the most effective ways to protect mine workings. To solve the problems, it is necessary to reveal the physical essence of deformation effects and determine their influence on the mechanical characteristics of protective structures made of broken rock, which will ensure stability of side rocks and development mine workings in a coal mass.

Various technologies for the formation of filling masses in the mined-out space are known for the use of complete or partial backfilling [1]-[3].

The world practice of using the methods of mined-out space backfilling [4]-[8] shows that the pneumatic and gravity methods are the most appropriate ones [2], [9]. Ensuring the stability of development mine workings in such conditions requires searching for effective protective measures [10], [11]. Gob pack is one of them [9]. However, backfilling by laying gob packs has some disadvantages. In particular, it is significant depression of rock packs after their contact with the roof. Moreover, it is low load-bearing capacity of protective structures stipulated by the fact that backfill material will spread to the sides under the action of load due to the lack of lateral supports.

It is believed [12], [13] that monitoring of the convergence of side rocks on their contour is a more important aspect in supporting development mine workings along the length of the working area. Therefore, having certain physico-mechanical properties, backfill masses after their compression will make it possible to limit displacement of side rocks in the mined-out space of a coal mass.

To assess bearing capacity of protective structures made of broken rock, it is recommended to consider a deformation modulus when calculating their stability [14]. It should be noted that the changes in deformation modulus while static load of backfill materials help assess their elastic and residual deformations, affecting the rigidity of structures.

Application of solidifying backfilling of the mined-out space ensures completeness of the mineral extraction and safety of mining operations. When using this method, deformations of side rocks decrease, while bearing capacity of protective structures during solidifying increases [15]. However, a depth of mining operations is the main criterion regulating the strength of backfill masses (rock backs) made of solidifying mixtures.

Assessment of the stability of protective structures designed to support side rocks and mine workings in a coal mass, which is based on the study of their deformation effects influencing the mechanical properties, is a topical scientific task. Disclosure and study of the physical essence of deformation effects is an important component of the analysis of stability of protective structures carried out to solve a problem of improving miners' safety and coal mining efficiency.

The purpose of the study is to reveal the physical essence of the dualistic (double) nature of deformation effects and their influence on the mechanical properties of protective structures made of broken rock while unloading coal-bearing masses to ensure stability of side rocks and operational con-

ditions of development mine workings within the working areas of coal mines.

To achieve the goal, following tasks were set:

- to investigate the essence of deformation effects and their influence on the mechanical properties of broken rock in terms of static load of protective structures under uniaxial compression with the possibility of lateral expansion of the source material;
- to study the deformation effects and their influence on the mechanical properties of broken rock under static load conditions during compressive stress of the source material;
- to perform a comparative analysis of the deformation characteristics of flexible supports made of broken rock under different compression conditions and draw a conclusion regarding manifestation of duality in the deformation effects to assess a stress-strain state of protective structures.

2. Methods

The object of the study is deformation processes and effects in flexible supports made of broken rock under static load to control a state of side rocks in a coal mass with the development mine workings. Deformation properties of flexible broken-rock supports were studied under laboratory conditions and evaluated basing on the analysis of the states of models of protective structures under uniaxial compression of the backfill material with the possibility of its lateral expansion and compressive stress. To do that, broken rock of different granulometric composition was used in the models.

When selecting broken rock for experimental samples, following ratio was used [16]:

$$\operatorname{tg} \rho_m = \operatorname{tg} \rho_n, \quad (1)$$

where:

$\rho_m = \rho_n$ – internal friction angle of the material of a model and a full-scale sample, degree.

To study the deformation characteristics of backfill materials, broken rock of following fraction sizes was used:

- (0.1-5) mm, of non-homogeneous (in terms of particle size) granulometric composition;
- (4-5) mm, being 100% of the volume of the backfill material;
- (3-4) mm, being 100% of the volume of the backfill material;
- (2-3) mm, being 100% of the volume of the backfill material;
- (1-2) mm, being 100% of the volume of the backfill material;
- (0.1-1) mm, being 100% of the volume of the backfill material.

The percentage composition of fractions in the source material of broken rock was determined after screening and counterbalance weighing with an accuracy up to 0.01 g. The source material was screened through a set of sieves with the holes of 5, 4, 3, 2, 1, and 0.1 mm [17]. Laboratory samples dried to a constant weight were used. Bulk density of broken rock $\rho_{b.d.}$ (kg/m³) was determined according to [17]. The results of laboratory studies of screening analysis of broken rock, its bulk density $\rho_{b.d.}$ (kg/m³), and coefficient of transverse deformation ν are given in Table 1.

Table 1. Results of laboratory studies of the screening analysis of broken rock and its correspondence to the bulk density $\rho_{b.d.}$ (kg/m³) and coefficient of transverse deformation ν

No.	Fraction size, mm	Bulk density ($\rho_{b.d.}$), kg/m ³	Coefficient of transverse deformation (ν)
1	0.1-5	1820	0.25
2	4-5	1680	0.28
3	3-4	1720	0.27
4	2-3	1860	0.29
5	1-2	1880	0.3
6	0.1-1	1920	0.32

Figure 1 shows a general view of the Π -50 hydraulic press for determining deformation characteristics of the broken-rock backfill material under static load.

**Figure 1. General view of hydraulic press Π -50 for determining deformation characteristics of the backfill material made of broken rock**

The deformation characteristics of a flexible support with the possibility of lateral expansion of the source material under static uniaxial compression was studied in terms of experimental samples of broken rock with different granulometric composition (Table 1). The source material was placed in a fabric shell. Sample dimensions are as follows: width is $b = 0.04$ m; length is $l = 0.08$ m; and initial height is $h_0 = 0.04$ m. The experimental samples were placed between the roof and the floor, which were made of a sand-cement mixture in the form of a slab model. At the same time, the identity of the equilibrium equations of the natural sample and the model was ensured [16]. To guarantee the mechanical similarity of the model and the full-scale sample, the equality of weight parameters was rejected, which is quite acceptable [18]. The modeling scale was 1:25. Table 2 shows characteristics of the roof and floor model materials.

Table 2. Characteristics of the roof and floor model materials

Object	Material	Density (γ), kg/m ³	Ultimate compressive strength (σ_{st}), MPa
Model	Sand-cement mixture	1600	1.33
Prototype	Aleurolite	2300	48

To determine the compressive properties of the backfill material, a steel cylinder, filled with broken rock of different granulometric composition, was used (Table 1). The cylinder diameter is $d_c = 0.075$ m; its height is $h_c = 0.075$ m. The initial height of the bedrock is $h_0 = 0.063$ m.

The general appearance of the experimental samples is shown in Figure 2. The experimental samples were placed between the metal plates of Π -50 press and subjected to a static load. During the experiments, deformation of the samples Δh (m) from the compressive force F (MPa) was recorded.

**Figure 2. Experimental models for studying deformation properties of broken rock under static load conditions: (a) for uniaxial compression with lateral expansion; (b) for compressive stress of the source material; 1 – fabric shell on the broken rock; 2 – steel cylinder; 3 – plunger; 4 – broken rock; b – sample width, m; l – sample length, m; h – sample height, m**

In terms of uniaxial compression, relative deformation λ of the experimental samples was determined according to Expression [19]:

$$\lambda = \frac{\Delta h}{h_0}. \quad (2)$$

Stiffness C (N/m) of the experimental samples was determined according to Expression [20]:

$$C = \frac{F}{\Delta h}. \quad (3)$$

Relative change in volume δV of the experimental samples under static load in terms of uniaxial compression with the possibility of lateral expansion of broken rock was determined according to Expression [21]:

$$\delta V = (1 - 2\nu) \cdot \mu, \quad (4)$$

where:

μ – Poisson's ratio.

Under static load, the deformed body changes its size in terms of uniaxial compression. The longitudinal dimension decreases, and the transverse dimension increases. Based on this, compaction factor $k_{con.}$ of broken rock was set through the parameter δV during static load of the experimental samples in terms of their uniaxial compression with lateral expansion of the source material.

When the broken rock is compressed in a compression device (cylinder), the diameter of the experimental sample does not experience any changes. Therefore, the relative vertical deformation of the source material is equal to the relative change in volume [22]:

$$\delta V = \frac{\Delta V}{V} = \frac{\Delta h}{h}. \quad (5)$$

It should be noted that compressive stress is a special case of triaxial compression with additional boundary conditions, which imply the impossibility of lateral expansion of the source material. In such conditions, the compaction factor of the broken rock k_{con} was calculated by the ratio of the volume occupied by the broken rock before its compaction to the volume of this rock after compaction [17], [22].

In case of uniaxial compression, mechanical stress σ (MPa) is considered to be pressure [18] and is defined as:

$$\sigma = \frac{F}{S}. \quad (6)$$

Modulus of deformation E_g (N/m²) of protective structures was determined basing on Hooke's law by Expression [23]:

$$E_g = \sigma \frac{h_0}{\Delta h}. \quad (7)$$

The specific potential energy of deformation of the experimental samples U (J/m³) was determined as in [24]:

$$U = \frac{\sigma^2}{2E_g}. \quad (8)$$

A void factor M_0 (%) of the backfill material was determined by the calculation based on the preset values of the

source material density ρ_b (kg/m³) and source material bulk density ρ according to Expression [17]:

$$M_0 = \left(1 - \frac{\rho_b}{\rho}\right) \cdot 100. \quad (9)$$

A void factor M (%) after compression was determined by changing the parameter δV .

It was assumed that in the deformation of experimental samples, the work of external forces is spent on changing their shape and volume. It was taken into account that the internal potential energy of deformation has critical levels; during the transition, the experimental samples change a stress-strain state [25], [26].

3. Results and discussion

3.1. Deformation effects of the support made of broken rock in terms of uniaxial compression

This subsection identifies influence of deformation effects on the mechanical properties of a support made of broken rock, being under uniaxial compression and static load.

Table 3 shows the experimental data of the static load of a support made of broken rock of different granulometric composition after compaction of the source material as a result of its uniaxial compression and lateral expansion.

Table 3. Experimental data of the static load of a support made of broken rock of different granulometric composition after compaction of the source material as a result of uniaxial compression and lateral expansion

No.	Fraction size, mm	Compressive force (F), MPa	Longitudinal deformation (Δh), m	Relative deformation (λ)	Relative volume change (δV)	Stiffness ($C \cdot 10^6$), N/m	Mechanical stress (σ), MPa	Deformation modulus (E_g) (N/m ²)	Specific potential energy of deformation ($\sigma^2/2E_g$), MJ/m ³	Compaction factor (k_{con})
1	0.1-5	118	0.026	0.65	0.32	4.53	18.4	28.1	5.8	1.47
2	4-5	120	0.025	0.62	0.28	4.28	18.7	29.9	5.79	1.4
3	3-4	125	0.024	0.6	0.27	5.2	19.5	32.3	5.85	1.37
4	2-3	121	0.019	0.47	0.2	6.36	18.9	39.6	4.34	1.25
5	1-2	116	0.016	0.4	0.16	7.25	18.1	45.2	3.62	1.19
6	0.1-1	112	0.014	0.35	0.12	8.0	17.5	49.8	2.97	1.13

Figure 3 demonstrates graphs of changes in relative deformation λ of a flexible support made of broken rock of different granulometric density $\rho_{b.d}$ (kg/m³) and its longitudinal deformation Δh (m).

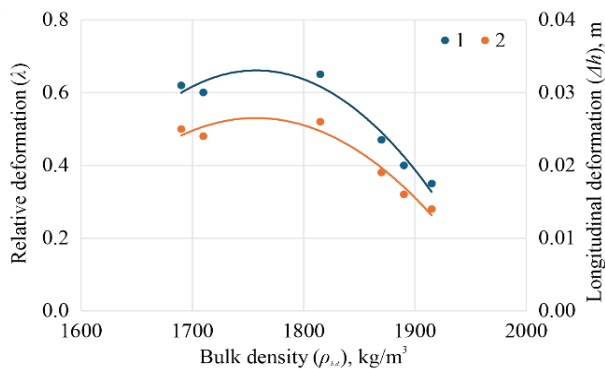


Figure 3. Graphs of changes in relative deformation λ of a flexible support made of broken rock of different granulometric density $\rho_{b.d}$ (kg/m³) and its longitudinal deformation Δh (m) in terms of static load at uniaxial compression of the backfill material with possible lateral expansion: 1 – λ ; 2 – Δh (m)

In terms of uniaxial compression of the experimental samples, maximum value of their relative deformation $\lambda = 0.65$ and longitudinal deformation $\Delta h = 0.026$ m is recorded under static load of broken rock of bulk density being $\rho_{b.d} = 1820$ kg/m³ (Fig. 3). The backfill material at this bulk density is represented by an inhomogeneous (by particle size) fraction of the source material (0.1-5) mm. When compressing large fraction (4-5) mm of broken rock with bulk density of $\rho_{b.d} = 1680$ kg/m³, relative deformation of the experimental sample is $\lambda = 0.62$, and its longitudinal deformation is $\Delta h = 0.025$ m. For the fine fraction of broken rock (0.1-1) mm, with a bulk density of $\rho_{b.d} = 1920$ kg/m³, relative deformation is $\lambda = 0.35$, and longitudinal deformation is $\Delta h = 0.014$ m. Between the considered parameters, there is a quadratic functional dependence with a correlation coefficient of $R = 0.86$ (Fig. 3).

3.2. Deformation effects of a support made of broken rock in terms of compressive stress

This subsection analyzes the influence of deformation effects on the mechanical properties of a support made of broken rock, which was in the conditions of compressive stress and static load.

Table 4 shows the experimental data of the static load of a support made of broken rock of different granulometric composition in terms of compressive stress.

Figure 4 shows graphs of changes in relative deformation λ and longitudinal deformation Δh (m) of a support made of broken rock of different granulometric density $\rho_{b.d.}$ (kg/m³) of the source material. It was recorded that during compression of broken rock with a bulk density of $\rho_{b.d.} = 1820$ kg/m³, relative deformation of the experimental samples is $\lambda = 0.38$,

and longitudinal deformation is $\Delta h = 0.024$ m. When the bulk density of broken rock decreases to the value of $\rho_{b.d.} = 1680$ kg/m³, relative deformation decreases to $\lambda = 0.31$, and longitudinal deformation – to $\Delta h = 0.02$ m.

As the bulk density increases to $\rho_{b.d.} = 1920$ kg/m³, relative deformation decreases to $\lambda = 0.14$, and longitudinal deformation – to $\Delta h = 0.009$ m. There is a quadratic dependence between the parameters under consideration (Fig. 4).

Table 4. Experimental data of the static load of a support made of broken rock of different granulometric composition after compaction of the source material in terms of compressive stress

No.	Fraction size, mm	Compressive force (F), MPa	Longitudinal deformation (Δh), m	Relative deformation (λ)	Relative volume change (δV)	Stiffness ($C \cdot 10^6$), N/m	Mechanical stress (σ), MPa	Deformation modulus (E_g) (N/m ²)	Specific potential energy of deformation ($\sigma^2/2E_g$), MJ/m ³	Compaction factor ($k_{con.}$)
1	0.1–5	155	0.024	0.38	0.38	6.45	35.1	91.9	6.7	1.59
2	4–5	130	0.02	0.31	0.31	6.5	29.5	92.9	4.68	1.47
3	3–4	112	0.018	0.28	0.28	6.2	25.4	88.9	3.62	1.39
4	2–3	92	0.015	0.23	0.23	6.13	20.9	87.7	2.49	1.3
5	1–2	86	0.012	0.19	0.19	7.1	19.5	102.3	1.85	1.23
6	0.1–1	75	0.009	0.14	0.14	8.3	17.0	119	1.21	1.16

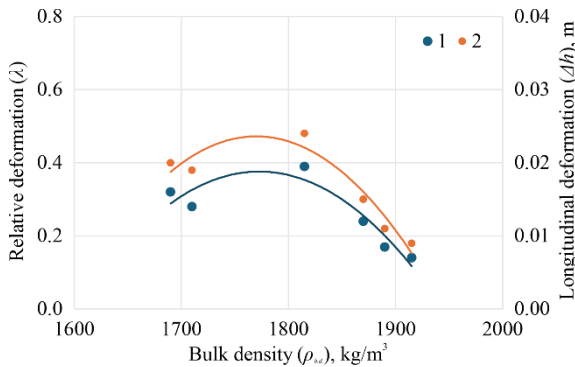


Figure 4. Graphs of changes in relative deformation λ of a flexible support made of broken rock of different bulk density $\rho_{b.d.}$ (kg/m³) and its longitudinal deformation Δh (m) in terms of static load during compressive stress of the backfill material: 1 – λ ; 2 – Δh (m)

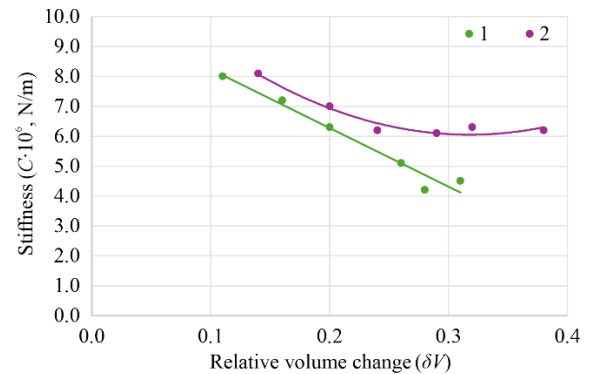


Figure 5. Graphs of the formation of stiffness C (N/m) of a flexible broken-rock support under different compression conditions from the relative change in volume δV of the backfill material: (1) under uniaxial compression; (2) under compressive stress

3.3. Comparative analysis of the deformation properties of flexible supports made of broken rock under different compression conditions

This subsection represents the results of a comparative analysis of the deformation effects that occur during the compression of flexible supports made of broken rock under different compression conditions. Their influence on the mechanical properties of supports with regard to the manifestation of duality in deformation effects was identified.

Figure 5 shows graphs of the formation of stiffness C (N/m) of a flexible support made of broken rock under different compression conditions from the relative change in volume δV of the backfill material. During uniaxial compression of the experimental sample with a change in the relative volume from $\delta V = 0.12$ to $\delta V = 0.32$, the stiffness decreases from $C = 8.0 \cdot 10^6$ N/m to $C = 4.53 \cdot 10^6$ N/m (Fig. 5, curve 1). There is a linear dependence between the studied parameters of the form $C = -19.0484 \delta V + 10.2226$ with the correlation coefficient being $R = 0.97$. An average approximation error is 1.31%.

In terms of compressive stress of the experimental sample with a change in the relative volume from $\delta V = 0.14$ to $\delta V = 0.38$, stiffness of the backfill material decreases from $C = 8.3 \cdot 10^6$ N/m to $C = 6.45 \cdot 10^6$ N/m (Fig. 5, curve 2).

There is quadratic dependence between the investigated parameters of the form $C = 79.6892 \delta V^2 + 48.0396 \delta V + 13.3522$ with the correlation coefficient being $R = 0.948$. An average approximation error is 2.79%.

Figure 6 shows graphs of changes in relative deformation λ of a support made of broken rock under static load in terms of different conditions of compression from the specific potential energy of deformation $\sigma^2/2E_g$. It was recorded that under conditions of uniaxial compression with an increase in relative deformation of the experimental samples from $\lambda = 0.35$ to $\lambda = 0.65$, the strain energy density increases from $\sigma^2/2E_g = 2.97$ MJ/m³ to $\sigma^2/2E_g = 5.8$ MJ/m³ (Fig. 6, curve 1).

In terms of the backfill material compression, with an increase in relative deformation from $\lambda = 0.14$ to $\lambda = 0.38$, the deformation energy density increases from $\sigma^2/2E_g = 1.21$ MJ/m³ to $\sigma^2/2E_g = 6.7$ MJ/m³ (Fig. 6, curve 2).

Figure 7 demonstrates graphs of changes in modulus of deformation E_g of a flexible support depending on a function of compaction coefficient $k_{con.}$ of broken rock at static load. In terms of uniaxial compression, with an increase in the compaction factor from $k_{con.} = 1.13$ to $k_{con.} = 1.47$, deformation modulus increases from $E_g = 28.1$ MPa to $E_g = 49.8$ MPa (Fig. 7, curve 1).

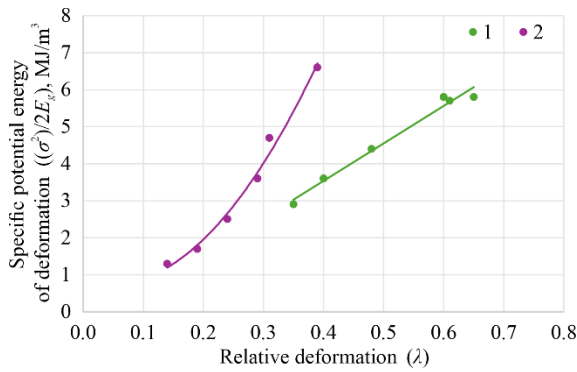


Figure 6. Graphs of changes in relative deformation λ of a broken-rock support made under static load: (1) under uniaxial compression with lateral expansion of the source material; (2) under compressive stress from the specific potential energy of deformation $\sigma^2/2E_g$ (MJ/m³)

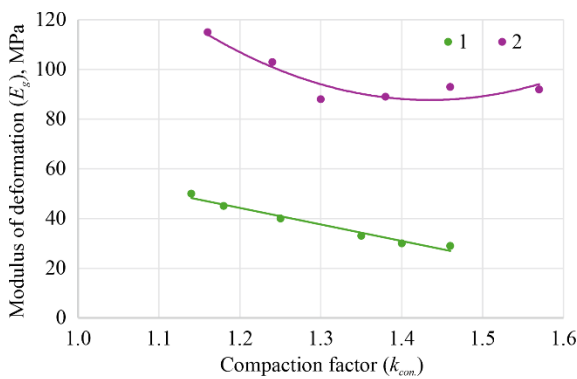


Figure 7. Graphs of changes in deformation modulus E_g of a flexible support depending on compaction factor $k_{con.}$ of broken rock under static load: (1) under uniaxial compression; (2) under compressive stress

When a flexible support is subjected to static load in terms of compression, within the range of the compaction

factor of broken rock $1.16 \leq k_{con.} \leq 1.59$, the deformation modulus decreases from $E_g = 119$ MPa to $E_g = 87.7$ MPa, and then increases to $E_g = 92.9$ MPa, which is associated with the increase in structure resistance after maximum compaction of broken rock ($k_{con.} = 1.59$) (Fig. 7, curve 2).

The void factor of the backfill material depends on the granulometric composition of broken rock. Table 5 shows the experimental data for determining void factor M_0 (%) before compression and M (%) after compression of the backfill material.

Table 5. Experimental data on determining void factor M_0 (%) before compression and M (%) after compression of the different-fraction backfill material

Fraction size, mm	Void factor before compression (M_0), %	Void factor after compression (M), %	
		Uniaxial	Compressive
0.1-5	15	10.1	9.3
4-5	20	14.4	13.8
3-4	18	13.1	12.9
2-3	13	10.4	10.0
1-2	10	8.4	8.1
0.1-1	6	5.3	5.1

The data in Table 5 reveal that, depending on the compression conditions, a void factor of the backfill material decreases by 0.7-5.7%. The maximum void-factor reduction value of 4.9% was recorded during uniaxial compression of broken rock of the (0.1-5) mm fraction and 5.7% during compressive stress of the same rock fraction. The void factor value depends on the ratio of particles of different sizes as well as on the compaction degree of backfill material.

For a comparative analysis of the deformation characteristics of flexible supports, the backfill material of fraction (0.1-5) mm, being in different compression conditions, was considered. Table 6 shows the experimental data of the static load of broken rock under uniaxial compression.

Table 6. Experimental data of the static load of a support made of broken rock of (0.1-5) mm fraction in terms of uniaxial compression with lateral expansion of the source material

Compressive force (F), MPa	Longitudinal deformation (Δh), m	Relative deformation (λ)	Mechanical stress (σ), MPa	Relative volume change (δV)	Stiffness ($C \cdot 10^6$), N/m	Deformation modulus (E_g), N/m ²	Compaction factor ($k_{con.}$)
10	0.003	0.07	1.56	0.035	3.3	20.8	1.04
20	0.008	0.2	3.12	0.1	2.5	15.6	1.11
30	0.01	0.25	4.68	0.12	3.0	18.7	1.13
50	0.015	0.37	7.8	0.18	3.3	20.8	1.22
70	0.02	0.5	10.9	0.25	3.5	21.8	1.33
80	0.023	0.57	12.5	0.28	3.47	21.7	1.39
100	0.024	0.6	15.6	0.3	4.16	26.0	1.43
110	0.025	0.62	17.1	0.31	4.4	27.3	1.45
118	0.026	0.65	18.4	0.32	4.53	28.3	1.47

Table 7 shows the experimental data of the static load of broken rock in terms of compressive stress.

According to the defined experimental data, dependence of the change in height h (m) of the experimental samples on the value of external force F (MPa) was constructed (Fig. 8).

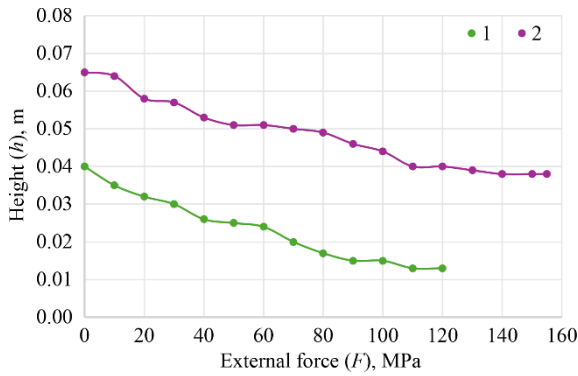
It was recorded that along with the increasing external force from $F = 5$ MPa to $F = 110$ MPa, the height of the experimental sample under uniaxial compression decreases from $h = 0.04$ m to $h = 0.015$ m (Fig. 8, curve 1). Under compressive stress in the same interval of changes in the

external load, the height of the experimental sample changes from $h = 0.063$ m to $h = 0.04$ m (Fig. 8, curve 2).

Figure 9 shows graphs of a relative change in volume δV of the backfill material under different load conditions depending on a function of compaction factor $k_{con.}$ of broken rock and stiffness C (N/m) of a flexible support. It is recorded that for the experimental sample, being under uniaxial compression with an increasing compaction factor from $k_{con.} = 1.04$ to $k_{con.} = 1.47$, the relative change in the backfill material volume is within the value range of $0.035 \leq \delta V \leq 0.32$.

Table 7. Experimental data of the static load of a support made of broken rock of (0.1-5) mm fraction in terms of source material compression

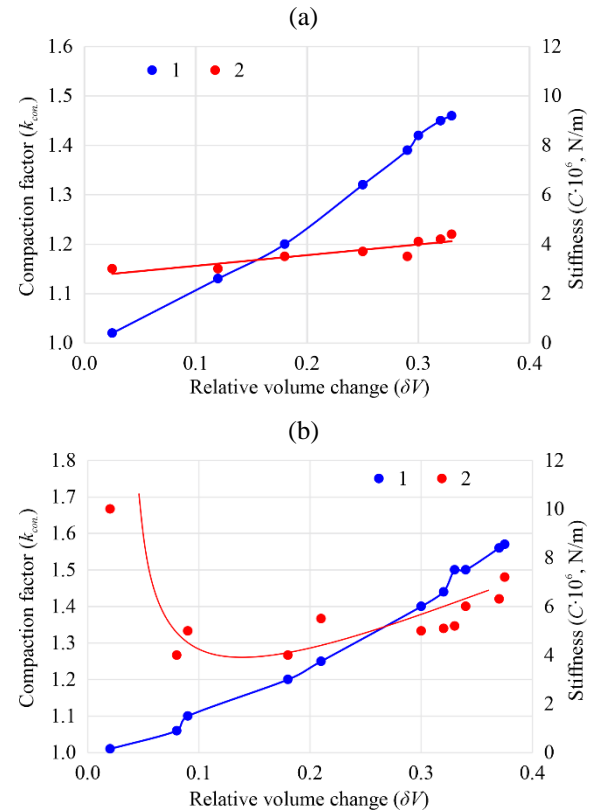
Compressive force (F), MPa	Longitudinal deformation (Δh), m	Relative deformation (λ)	Mechanical stress (σ), MPa	Relative volume change (δV)	Stiffness ($C \cdot 10^6$), N/m	Deformation modulus (E_g) (N/m ²)	Compaction factor ($k_{con.}$)
10	0.001	0.01	2.26	0.01	10.0	142.4	1.01
20	0.005	0.08	4.53	0.08	4.0	57.1	1.08
30	0.006	0.09	6.8	0.09	5.0	71.4	1.1
50	0.012	0.19	11.3	0.19	4.16	59.3	1.23
70	0.013	0.2	15.8	0.2	5.38	76.5	1.25
80	0.014	0.22	18.1	0.22	5.7	81.4	1.28
100	0.019	0.3	22.6	0.3	5.26	75.0	1.43
110	0.021	0.33	24.9	0.33	5.23	74.7	1.5
120	0.022	0.35	27.2	0.35	5.45	77.9	1.53
140	0.023	0.36	31.7	0.36	6.1	86.8	1.57
150	0.024	0.38	34.0	0.38	6.25	89.2	1.59
155	0.024	0.38	35.1	0.38	6.45	92.1	1.59

**Figure 8. Graphs of changes in height h (m) of a support made of broken rock of (0.1-5) mm fraction: (1) under uniaxial compression with lateral expansion of the source material; (2) under compression from the magnitude of the external force F (MPa)**

At the same time, the sample stiffness decreases from $C = 3.3 \cdot 10^6$ N/m to $C = 2.5 \cdot 10^6$ N/m, then gradually increases to the value of $C = 4.53 \cdot 10^6$ N/m as the compressive load increases (Fig. 9a). When compressing the experimental sample, with an increasing compaction factor from $k_{con.} = 1.01$ to $k_{con.} = 1.59$, the relative change in the backfill material volume is within the range of $0.01 \leq \delta V \leq 0.38$. At the same time, the sample stiffness decreases from $C = 10 \cdot 10^6$ N/m to $C = 4.0 \cdot 10^6$ N/m, and then gradually increases to the value $C = 6.45 \cdot 10^6$ N/m (Fig. 9b).

Figure 10 shows graphs of changes in relative deformation λ and volume δV of a flexible support under static load depending on the function of compaction factor $k_{con.}$ of broken rock. When analyzing a change in relative deformation λ of the experimental samples, the $k_{con.}$ parameter growth was recorded while λ increasing, which reflects the physical essence of a compaction mechanism of the backfill material (Fig. 10 a).

It was specified that when a compaction factor increases from $k_{con.} = 1.13$ to $k_{con.} = 1.59$, the relative volume change increases from $\delta V = 0.12$ to $\delta V = 0.38$ (Fig. 10 b). A logarithmic dependence of the form $\delta V = 0.0313 + 0.7473 \ln k_{con.}$ is identified between the analyzed parameters δV and $k_{con.}$ with the correlation coefficient $R = 0.99$. An average approximation error is 1.31%. As a result of the conducted studies, the availability of dualistic effects of deformations and their influence on the mechanical properties of broken-rock experimental samples was established.

**Figure 9. Graphs of a relative change in volume δV of a support made of broken rock of (0.1-5) mm fraction: (a) under uniaxial compression with lateral expansion of the source material; (b) under compressive stress of the source material depending on compaction factor $k_{con.}$ and stiffness $C \cdot 10^6$ (N/m); 1 – $k_{con.}$; 2 – $C \cdot 10^6$ (N/m)**

The experimental samples were models of flexible protective structures of development mine workings. Under the action of external force F (MPa), a sample was deformed, which simulated the real state of the protective structure. The potential energy of the deformed body (Expression (8)) was considered as the equivalent of the work spent on uniaxial compression or compressive stress. When protective structures were deformed, their volume and shape changed. It was conventionally believed that there was a dualistic bifurcation of the external forces operation, which was spent on changing the volume and changing the shape of the protective structure body.

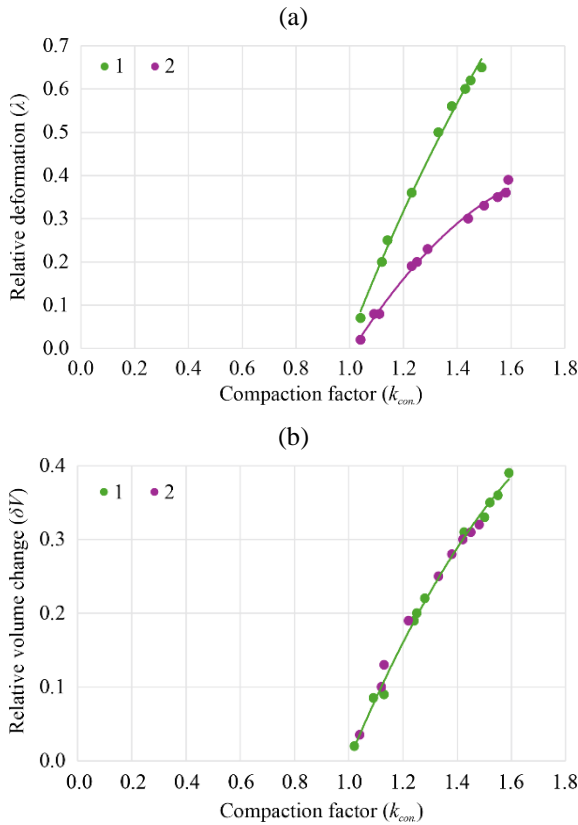


Figure 10. Graphs of changes in (a) relative deformation λ and (b) relative change in volume δV of a flexible support depending on its compaction factor k_{con} under static load in terms of uniaxial compression (1) and compressive stress (2)

The support stiffness (Expression (3)) was related to the amount of its deformation Δh (m) under static load. By registering a relative change in volume δV (Expression (4)), the behavior of the deformed body was evaluated.

Under static load for a flexible support made of broken rock in terms of uniaxial compression with lateral expansion of the backfill material, the longitudinal size of the deforming body decreases, and the transverse size, on the contrary, increases. Longitudinal deformations determine depression of a flexible support and changes in the volume (Table 3). After reaching the boundary value of the compaction factor of broken rock ($k_{con} = 1.47$), the transverse expansion of the support occurs due to the backfill material extrusion beyond the supporting column. In such a situation, transverse deformations reveal the effect of changing the body shape as a maximally compacted volume of the backfill material.

When the broken rock is subjected to static load under compressive stress, the longitudinal size of the deformed body changes. After reaching the maximum value of the compaction factor ($k_{con} = 1.59$), the backfill material transits into a stressed state. In such a situation, longitudinal deformations are the result of a decreasing void factor of the backfill material and a change in volume; they determine the broken rock depression (Table 4).

In this study, deformation modulus E_g (N/m²) characterizes the elastic and residual deformations of the backfill material at static load under different compression conditions. Under the action of an external load, residual deformations occur in terms of uniaxial compression as a result of lateral expansion of broken rock. In terms of compressive

stress, it is when broken rock is compacted. High values of the modulus of deformation $E_g = 49.8$ N/m² are achieved during compression of the backfill material when it contains 100% of fine rock fraction. In such conditions, the minimum values of the compaction factor $k_{con} = 1.13$ of the source material are fixed.

Under compressive stress of the backfill material, with the availability of 100% of fine rock fraction in its composition, the deformation modulus is $E_g = 119$ MPa at the minimum value of the compaction factor being $k_{con} = 1.16$. The increase in the resistance of protective structures occurs after the maximum compaction of broken rock with the growth of their deformation modulus. The modulus of deformation characterizes the backfill material rigidity.

It was recorded that in terms of uniaxial compression of broken rock with an increasing specific potential energy of deformation, there is an increase in the relative deformation of protective structures according to a linear dependence (correlation coefficient is 0.97) (Fig. 6, curve 1), which affects significantly the stability of the supporting column of the backfill material. In case of compressive stress of broken rock, the system parameters reach the boundary values, due to reaching the maximum compaction ratio. In such conditions, the support changes its behavior, which affects its stress-strain state. The support stability increases. There is a functional dependence in the form of a hyperbola between the change in the specific potential energy of the deformation of security structures and their relative deformation (correlation coefficient is 0.98) (Fig. 6, curve 2).

The change in stiffness of the backfill material occurs as a result of its compaction in the total broken rock volume due to rearrangement of fractions, filling of cavities and additional breaking of the material under static load. The hardness of the backfill material at its maximum compaction reflects the flexible support reaction to the external influence (load). However, the rigidity of structures is not a constant value and increases with the growing value of a compressive force. Its compaction factor should be considered as a criterion for evaluating hardness of the backfill material made of broken rock.

Void factor M_0 (%) of the backfill material depends on the granulometric composition of the broken rock. As a result of compression, the void factor changes to M values (%). In case when the backfill material is represented by a homogeneous fine fraction (0.1-1) mm, its deformation occurs due to elastic compression of the broken rock. For a homogeneous fraction of broken rock (4-5) mm, during the backfill material formation, elastic compression of the particles occurs until the moment of their breaking. Then they are repackaged in the total volume of broken rock. With an inhomogeneous granulometric composition (0.1-5) mm of broken rock, there is a mutual displacement of the particles relative to each other with the maximum change in the void (4.7-4.9%) and compaction ($k_{con} = 1.47$ or $k_{con} = 1.59$) factors (Figs. 9, 10).

While comparing the compaction factor data, the difference in the deformation characteristics of broken rock under uniaxial compression and compressive stress reaches two or more times, depending on the degree of source material homogeneity (Figs. 6, 10). This is related to the distribution of internal potential energy of protective structures deformation during compression (Fig. 6). For example, with the values of compaction factor of broken rock $k_{con} = 1.4$, the relative change in the backfill material volume in the protective

structure is approximately $\delta V = 0.3$ (Fig. 10b). Relative deformation of the protective structure under uniaxial compression is equal to $\lambda = 0.6$ (Fig. 10a, curve 1), and under compressive stress, it is $\lambda = 0.3$ (Fig. 10a, curve 2). Here, the modulus of deformation under uniaxial compression is equal to $E_g = 30 \text{ N/m}^2$ (Fig. 7, curve 1), and under compressive stress, it is $E_g = 88 \text{ N/m}^2$ (Fig. 7, curve 2). The specific potential energy of deformation under uniaxial compression is equal to $\sigma^2/2E_g = 5.72 \text{ MJ/m}^3$ (Fig. 6, curve 1), and during compressive stress, it is $\sigma^2/2E_g = 4.0 \text{ MJ/m}^3$ (Fig. 6, curve 2). That is, under compressive stress of broken rock, the specific potential energy of deformation is approximately by 30% more than under its uniaxial compression with the possibility of lateral expansion of the backfill material. Such a difference is recorded due to compaction or shape transformation under different compression conditions.

Thus, the deformation characteristics of protective structures of development mine workings show a dualistic (dual) nature of effects influencing the mechanical properties of backfill material made of broken rock. Such a dualistic ability of backfill masses to respond to the influence of various external factors manifested in the coal mass during its unloading expands possibilities of structures after their maximum compaction to limit the displacement of lateral rocks due to increasing resistance, which affects significantly the stability of development mine workings. Therefore, to evaluate the deformation characteristics of protective structures made of broken rock, it is necessary to use a compaction factor and granulometric (fractional) composition of the source rock material. It is required to take into consideration that different fractional compositions ensure qualitatively the backfill material compaction and forms the stress-strain state of the support under load.

4. Conclusions

Based on the research results, the physical essence of the dualistic (dual) nature of deformation effects was revealed. Their influence on the mechanical properties of protective structures made of broken rock was identified while coal mass unloading to ensure both stability of side rocks and safe operational condition of development mine workings within the working areas of coal mines. A regularity in the deformation effects of protective structures between compaction factor k_{con} of broken rock and a relative change in volume δV of the backfill material was specified. That made it possible to evaluate the stress-strain state and bearing capacity of protective structures for their certain load.

In terms of uniaxial static load of a flexible broken-rock support with the possibility of lateral expansion of the source material during compression, the change in a stress-strain state is a consequence of the transforming shape of the protective structures. When the bulk density of broken rock increases and when the relative change in its volume is within the range of $0.12 \leq \delta V \leq 0.32$, the deformation modulus and rigidity of protective structures change linearly reaching its maximum values when the backfill material contains 100% of fine fraction at a minimum relative change in volume. In case of protective structures made of broken rock of heterogeneous granulometric composition under static load, the deformation modulus and stiffness increase, when within the limits of relative changes in the backfill material volume being $\delta V \leq 0.32$, maximum compaction of the source mate-

rial ($k_{con} = 1.47$) and the supporting column strength of a flexible support are ensured.

Formation of the stress-strain state of a flexible support made of broken rock under the backfill material compression occurs after its compaction ($k_{con} = 1.59$) and relative changes in volume within the value range of $0.14 \leq \delta V \leq 0.38$, when there is a quadratic dependence between the change in protective structures stiffness and parameter δV . In this context, the dependence takes into account the changes in bulk density of the source material. In such conditions, the system parameters reach the boundary values that affects significantly the behavior of the security structure under load.

Basing of a comparative analysis of the deformation properties of protective structures, the essence of the dual nature of the deformation effects was established. It means that under static load of a flexible broken-rock support under uniaxial compression with the possibility of lateral expansion or compressive stress of the source material, when relative deformation of the support is taken into account, there is a logarithmic relationship between the compaction coefficient k_{con} and relative change in volume δV of the backfill material, which makes it possible to estimate the bearing capacity and stress-strain state of protective structures. Taking into account the granulometric composition of broken rock at the same values of its compaction factor k_{con} and a relative change in volume δV of the backfill material, the deformation modulus E_g of protective structures differs by 2.5 times depending on the compression conditions, which differs significantly their behavior under static load.

The research results can be used to substantiate the selection of a method for protecting development mine workings with flexible supports made of broken rock. To clarify the assessment of the bearing capacity of such structures, it is advisable to carry out specific field studies in mine conditions.

Author contributions

Conceptualization: DC, SP; Data curation: YeP; Formal analysis: DC, VG; Funding acquisition: SP; Investigation: DC, OD, YeP; Methodology: DC, SP, VG; Project administration: DC, SP, OD; Resources: OD; Supervision: OSh, OS; Validation: OSh, OS; Visualization: YeP; Writing – original draft: DC, SP, VG; Writing – review & editing: OSh, OS, OD, YeP. All authors have read and agreed to the published version of the manuscript.

Funding

This work was supported by the European Commission (grant number ENI/2019/413-664 “EDUTIP”).

Acknowledgements

The authors thank the staff of rock pressure laboratory of Donetsk National technical University for their assistance in the testing of experimental samples.

Conflicts of interests

The authors declare no conflict of interest.

Data availability statement

The original contributions presented in the study are included in the article, further inquiries can be directed to the corresponding author.

References

- [1] Buzilo, V.I., Sulaev, V.I., & Koshka, A.G. (2013). *Tekhnologiya obrabotki tonkikh plastov s zakladkoy vyrabotannogo prostranstva*. Donetsk: NGU.
- [2] Malashkevych, D.S. (2021). *Rozrobka tekhnologichnih skhem selektyvnoho vidpratsiuvannya plastiv iz zalysnenniam porody u vyroblenomu prostori*. Dnipro: Lizunov Press.
- [3] Salieiev, I. (2024). Organization of processes for complex mining and processing of mineral raw materials from coal mines in the context of the concept of sustainable development. *Mining of Mineral Deposits*, 18(1), 54-66. <https://doi.org/10.33271/mining18.01.054>
- [4] Witthaus, H., Gutberlet, K., & Junker, M. (2013). Stowing on longwall faces on the basis of experience acquired in the German coal mining industry. *Mining Report*, 75(6). <https://doi.org/10.1002/mire.201300422>
- [5] Huang, J., Tian, C., Xing, L., Bian, Z., & Miao, X. (2017). Green and sustainable mining underground coal mine fully mechanized solid dense stowing-mining method. *Sustainability*, 9(8), 1418. <https://doi.org/10.3390/su9081418>
- [6] Zhou, N., Jiang, H.Q., & Zhang, J.X. (2013). Application of solid backfill mining techniques for coal mine under embankment dam. *Mining Technology*, 122(4), 228-234. <https://doi.org/10.1179/1743286313Y.0000000042>
- [7] Zhang, Q., Zhang, J., Guo, S., Gao, R., & Li, W. (2015). Design and application of solid, dense backfill advanced mining technology with two pre-driving entries. *International Journal of Mining Science and Technology*, 25(1), 127-132. <https://doi.org/10.1016/j.ijmst.2014.12.008>
- [8] Malashkevych, D., Sotskov, V., Medyanik, V., & Prykhodchenko, D. (2018). Integrated evaluation of the worked-out area partial backfill effect of stress-strain state of coal-bearing rock mass. *Solid State Phenomena*, 277, 213-220. <https://doi.org/10.4028/www.scientific.net/ssp.277.213>
- [9] Jarkovich, A.I. (2015). Povyshenie ustoychivosti vyrabotok putem zakladki vyrabotannogo prostranstva. *Development of Deposits: Collection of Scientific Papers*, 9, 141-147.
- [10] Bondarenko, V., Symanovych, H., Barabash, M., Husiev, O., & Salieiev, I. (2020). Determining patterns of the geomechanical factors influence on the fastening system loading in the preparatory mine workings. *Mining of Mineral Deposits*, 14(1), 44-50. <https://doi.org/10.33271/mining14.01.044>
- [11] Bondarenko, V., Kovalevska, I., Symanovych, H., Barabash, M., & Salieiev, I. (2021). Principles for certain geomechanics problems solution during overworking of mine workings. *E3S Web of Conferences*, 280, 01007. <https://doi.org/10.1051/e3sconf/202128001007>
- [12] Tkachuk, O., Chepiga, D., Pakhomov, S., Volkov, S., Liashok, Y., Bachurina, Y., & Podkopaiev, S. (2023). Evaluation of the effectiveness of secondary support of haulage drifts based on a comparative analysis of the deformation characteristics of protective structures. *Eastern-European Journal of Enterprise Technologies*, 2(1)(122), 73-81. <https://doi.org/10.15587/1729-4061.2023.272454>
- [13] Chepiga, D., Bessarab, I., Hnatiuk, V., Tkachuk, O., Kipko, O., & Podkopaiev, S. (2023). Deformation as a process to transform shape and volume of protective structures of the development mine workings during coal-rock mass off-loading. *Mining of Mineral Deposits*, 4(17), 1-11. <https://doi.org/10.33271/mining17.04.001>
- [14] Petlovanyi, M., Malashkevych, D., Sai, K., & Zubko, S. (2020). Research into balance of rocks and underground cavities formation in the coal mine flowsheet when mining thin seams. *Mining of Mineral Deposits*, 14(4), 66-81. <https://doi.org/10.33271/mining14.04>
- [15] Kuz'menko, O., Petlyovany, M., & Stupnik, M. (2013). The influence of fine particles of binding materials on the strength properties of hardening backfill. *Annual Scientific-Technical Collection – Mining of Mineral Deposits*, 45-48. <https://doi.org/10.1201/b16354-10>
- [16] Nasonov, I.D. (1978). *Modelirovanie gornyykh protsessov*. Moskva, Rossiya: Nedra, 256 s.
- [17] Podkopaev, S.V., Gavrilsh, N.N., Deglin, B.M., Kamenec, V.I., & Zinchenko, S.A. (2012). *Laboratornyi praktikum z kursu "Mekhanika gornyykh porod"*. Donetsk, Ukraina: DonNTU.
- [18] Shashenko, O.M., Pustovoitenko, V.P., & Sdvyzhkova, O.O. (2016). *Geomehanika*. Kyiv, Ukraina: Novyi druk.
- [19] Podkopaiev, S., Gogo, V., Yefremov, I., Kipko, O., Iordanov, I., & Simonova, Yu. (2019). Phenomena of stability of the coal seam roof with a yielding support. *Mining of Mineral Deposits*, 13(4), 28-41. <https://doi.org/10.33271/mining13.04.028>
- [20] Czichos, H. (2013). Physics of failure. *Handbook of Technical Diagnostics*, 23-24.
- [21] Hnatiuk, V., & Kipko, O. (2023). Doslidzhennia protsesiv deformuvannya okhronnykh sporud pidhotovchykh hirnychkh vyrobok. *Naukovyi Visnyk DonNTU*, 2(11), 70-80.
- [22] Iordanov, I., Novikova, Yu., Simonova, Yu., Yefremov, O., Podkopaiev, Y., & Korol, A. (2020). Experimental characteristics for deformation of backfill mass. *Mining of Mineral Deposits*, 14(3), 119-127. <https://doi.org/10.33271/mining14.03.119>
- [23] Bachurin, L.L., Iordanov, I.V., Simonova, Y.I., Korol', A.V., Podkopaiev, Ye.S., & Kayun, O.P. (2020). Eksperymentalni doslidzhennia deformatsiynykh kharakterystyk zakladalnykh masyviv. *Tekhnichna Inzheneriya*, 2(86), 136-149. [https://doi.org/10.26642/ten-2020-2\(86\)-136-149](https://doi.org/10.26642/ten-2020-2(86)-136-149)
- [24] Meshkov, Yu.Ya. (2001). Koncepciya kriticheskoy plotnosti energii v k razrusheniya tverdykh tel. *Uspekhi Fiziki Metallov*, 2, 7-50.
- [25] Stupishin, L.U. (2014). Variational criteria for critical levels of internal energy of a deformable solid. *Applied Mechanics and Materials*, 578-579, 1584-1587. <https://doi.org/10.4028/www.scientific.net/AMM.578-579.1584>
- [26] Baranovskiy, E.M., & Moisyshyn, V.M. (2005). Energetichni teorii mitsnosti ta yikh vykorystannia v mekhanitsi hirnychkh porid. *Naukovyi Visnyk Natsionalnoho Tekhnichnogo Universytetu Nafty i Hazu*, 2(11), 26-32.

Дуалістичний ефект деформацій охоронних споруд гірничих виробок із подрібненої породи в умовах статичного навантаження

Д. Чепіга, С. Подкопаяєв, В. Гого, О. Шашенко, О. Скобенко, О. Демченко, Є. Подкопаяєв

Мета. Розкрити фізичну сутність дуалістичного (подвійного) характеру деформаційних ефектів та їх вплив на механічні властивості охоронних споруд із подрібненої породи в процесі розвантаження вуглепородного масиву для забезпечення стійкості бічних порід та експлуатаційного стану підготовчих виробок на виймкових дільницях вугільних шахт.

Методика. Моделювання деформаційних властивостей охоронних споруд із подрібненої породи виконувалося на експериментальних зразках в процесі їх статичного навантаження за умови одновісного стиснення із можливістю бічного розширення первісного матеріалу або його компресійного стиснення.

Результати. Виявлено дуалістичний ефект деформацій для умов одновісного стиснення охоронних споруд, за яким у них виникає комплексна трансформація об'єму і форми, як результат процесу відносної зміни об'єму закладного матеріалу. Спостережуване явище відбувається у межах $0.12 \leq \delta V \leq 0.32$ та значення коефіцієнту ущільнення подрібненої породи $1.13 \leq k_{con} \leq 1.47$, в залежності від граничного складу первісного матеріалу та його насипної щільності. Встановлено що в умовах, коли відбувається компресійне стиснення подрібненої породи, виникає ефект формування несучої здатності охоронних споруд, який спостерігається при відносній зміні об'єму закладного матеріалу $0.14 \leq \delta V \leq 0.38$ та досягненні коефіцієнту його ущільнення $1.16 \leq k_{con} \leq 1.59$. В залежності від ступеня однорідності закладного матеріалу охоронних споруд при порівнянні значень $k_{con,пр}$ проявляється дуалістичний (подвійний) ефект у різниці деформаційних характеристик подрібненої породи при одновісному і компресійному стисненні, що досягає двох і більше разів.

Наукова новизна. Встановлена закономірність, яка визначає зв'язок між коефіцієнтом ущільнення k_{con} подрібненої породи і відносною зміною об'єму (δV) закладного матеріалу, що дає можливість здійснити оцінку несучої здатності охоронних споруд, які знаходяться під статичним навантаженням у напружено-деформатійному стані.

Практична значимість. Результати досліджень можуть бути використані для обґрунтування вибору способу охорони підготовчих гірничих виробок піддатливими опорами із подрібненої породи. Для уточнення оцінки несучої здатності таких споруд доцільно проведення конкретних натурних досліджень у шахтних умовах.

Ключові слова: охоронна споруда, гірничі виробки, статичне навантаження, деформація, порода, несуча здатність

Publisher's note

All claims expressed in this manuscript are solely those of the authors and do not necessarily represent those of their affiliated organizations, or those of the publisher, the editors and the reviewers.